chapter II

Preparation & Characterization

Chapter - II

Section A: Preparation

2A.1 Introduction

The polycrystalline ferrites are usually prepared by mixing the constituent oxides, oxalates, carbonates etc. in proper proportions and sintering the mixture to a desired temperature. So that solid state reaction is brought out. The material so obtained is then ground to a fine powder, this powder is formed into the desired shape and size and again heated to a very high temperature to form homogeneous solid. A sintered polycrystalline specimen is not solid but contains large number of pores. The density, porosity and microstructure of the ferrite formed depends on the method of preparation. The purity of starting material, mixing, sintering temperature and time. These things affect the properties of final product. Also, microstructural factors such as grain size, defect concentration, pores, grain shape etc. considerably affect the properties of ferrites formed. Hence during preparation various factors are controlled to have a good quality ferrite.

2A.2 Ceramic Method of Preparation

The most widely used and accepted techniques is the classical ceramic method. In this method pure metal oxides are chosen. Then they are thoroughly and uniformly mixed with special techniques. This mixture is sintered for a prolonged time at a specified temperature in order to attain solid state reaction among the oxides and the formation of the compound.

The ceramic method consists of following stages -

1. Preparation of materials to form an intimate mixture so as to maintain the appropriate proportions of metal ions in the final product.
2. Presintering this mixture to initiate the formation of ferrite.
3. Powdering of the prepared sample and pressing or forming into the required shape to form pellets.
4. Sintering the pressed pellet at elevated temperature.

The flow chart of preparation method is given in Fig. 2.1.

2A.3(a) Method of preparation : Oxide method

This method is considered to be easiest. In this method highly pure oxides are mixed together in proper proportions. Generally this mixture is introduced in a

Fig. 2.1 Flow chart of the stages in the ferrite preparation

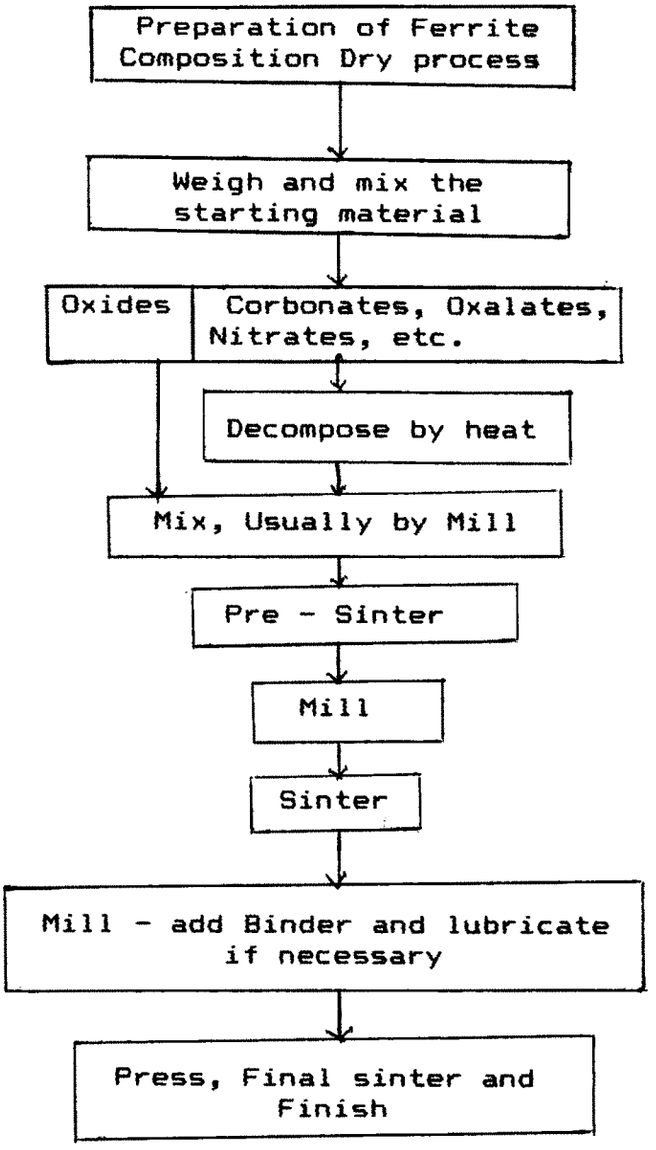

ball milling machine for several hours with acetone as mixing medium. After milling the mixture is dried and presintered. This presintered powder attains the solid state chemical reaction [1]. The presintered powder is again milled for an hour in acetone. The powder is then pressed into a suitable shape with the help of hydraulic pressure and finally sintered. The purity of oxides, particles size and shape are important for desired application [2].

2A.3b Decomposition method

Instead of using oxides as starting materials, one may start with salts such as carbonates, nitrates and oxalates. These salts are mixed in the requisite proportions pre-heating, usually in air, produces the oxides by thermal decomposition. the prepared oxide can undergo solid state reaction. Other details of this method is similar to that of oxide method.

2A.4 Pre-sintering

The process of presintering involves heating the intimate mixture of raw materials about 400 to 600° below its final firing temperature. The purpose of this method is to decompose carbonates and higher oxides thereby reducing the evolution of the gas in the final

sintering process [3]. It helps in homogenizing the material and control the shrinkage of the material that may otherwise occurs during final sintering. During this process the solid state reaction takes place and the raw materials partly react to produce the final compound. The rate of reaction depends upon the reactivity of the components as well as the presintering temperature.

2A.5 Pressing

The prefired powder is ground to a fine powder so as to reduce the particle size and to promote mixing of any unreacted oxides. The fine powder is usually mixed with some form of binder such as 1 % polyvinyl alcohol or 1 % ammonium alignate solution is used. The dried powder is then pressed to a required shape using a conventional die applying pressure of 8 to 10 tons/inch^2 from a hydraulic pump. Thus the pellets of required shape are formed.

2A.6 Hot Pressing

In this technique simultaneous application of external pressure with temperature enhances the densification [4,5] of the powder without grain growth. The continuous hot pressing technique gives fully dense

materials with the advantage of retaining the small grain size of the starting powder [6,7,8]. The microwave ferrite fabricated by this method have high density with average grain size at about Ø.5 μm. These materials are useful in high frequency applications.

2A.7 Sintering

For good quality of ferrites the grain size should be uniform. The pores should be intergranular and discontinuous grains. This can be achieved in the final sintering. The final sintering involves heating the pressed material to high temperature. The sintering is done to increase the density and hence to reduce porosity. It develops the final microstructure together with the correct oxygen content and the cation distribution. These depends upon the time and temperature of sintering [9].

2A.8.1 Actual Preparation of Ferrite Samples

The ferrite samples in the present study were prepared by the usual ceramic method.

(a) General formula

The general formula of composition is given by

$$Cu_xCo_{1-x}Al_{0.5}Fe_{1.5}O_4$$

Where x = Ø, Ø.2, Ø.4, Ø.6, Ø.8 and 1

(b) Starting materials

The raw or starting materials used for the preparation of ferrites are A.R. grade oxides such as cupric oxide (CuO), cobalt oxide (CoO), Ferric oxide (Fe_2O_3) and aluminium oxide (Al_2O_3).

(c) Weighing

In order to prepare each sample about 10 gms, the oxides were weighed to required molar composition using single pan, semi-microbalance. The required weighed oxides are mixed thoroughly in an agate mortar in acetone medium. This mixture is then allowed to dry and transferred it carefully to a clean and dry silica crucible. The same process is followed for all samples.

2A.8.2 Presintering and grinding

The mixture of each sample was presintered in a silica crucibles at 700 °C for 12 hours in air in glowbar furnace and then furnace was cooled slowly. The temperature of the furnace was measured with the help of chromel-alumel thermocouple which was calibrated by usual method. The presintered samples were ground in an agate-mortar for one and finally powder was collected in a clean glass tube.

2A.8.3 Pellet formation

To prepare a pellet, a small quantity (1gm) of powder was ground in acetone by adding few drops of polyvinyl acetate. The mixture was allowed to dry in air. The powder was poured into a punch die of 1 cm diameter and pressed in a hydraulic press with the pressure of the order of 6 to 8 tons per sq. inch for about 5 minutes. After removing the load, pellet was taken out from the die. In this way pellets for each sample were prepared.

2A.8.4 Final Sintering

The pellets so formed were kept on a thin platinum sheets and kept in a glowbar furnace at a temperature of 1000 °C about 30 hours in an air atmosphere for the completion of solid state reaction. Then the furnace was cooled at the rate of 80 °C/hour. Finally the pellets were polished so that opposite faces become exactly parallel to each other. Every pellet after polishing was carefully weighed on a microbalance and its dimensions were measured using thickness gauge and hence physical density is determined.

Section B - X-ray Diffraction Studies

2B.1 Introduction

The characterization of ferrite materials can be done by using x-ray diffraction. The simplest explanation of the observed diffraction pattern that results from the passage of x-rays through the crystal was first given by Bragg [1Ø]. X-ray diffraction technique is used

1. To study the crystal structure
2. To confirm the formation of solid state reaction
3. Determination of lattice constants interplaner distances, octahedral and tetrahedral site radii and bond lengths etc.
4. Observation of the impurity phase

Neutron diffraction as well as electron diffraction are also employed in determining the crystal structure of ferrites. The neutron diffraction study of ferrite is carried out by the number of workers [11,12].

2B.2 X-ray Diffraction Condition

Bragg put very stringent condition on x-rays for diffraction to occur. According to him diffraction is possible only when the wavelength of x-rays is

comparable with path difference. We have Bragg's conditions such as

$$2d \sin\theta = n\lambda \qquad \ldots \quad 2.1$$

Where n = order of diffraction

λ = wavelength of monochromatic x-ray

θ = glancing angle

d = interplaner distance

Since n = 1 is the least value of n, it corresponds to the first order reflection. Hence Bragg's law can be written as

$$\lambda = 2d \sin\theta$$

For cubic crystal,

$$d_{hkl} = \frac{a}{(h^2+K^2+l^2)^{1/2}} \qquad \ldots \quad 2.2$$

2B.3 X-ray Diffraction Method

Monochromatic x-rays of wavelength λ striking a 3 dimensional crystal at an arbitrary angle of incidence will not in general be reflected. To satisfy Bragg's condition and to cause diffraction we have to vary either wavelength (λ) or angle of incidence (θ). There are three methods of x-ray diffraction namely Laue method, Rotating crystal method and Powder method.

2B.3.1 Laue Method

Here a single crystal is kept stationary in a beam of x-rays of continuous wavelengths developed by Van Laue. The crystal selects a suitable wavelength and diffraction occurs from a plane with incident glancing angle θ. This method is suitable for crystal orientation, crystal symmetry and crystalline imperfections.

2B.3.2 Rotating crystal method

Scheibold and Polanyi developed this method in which a crystal is rotated about a fixed axis in a narrow beam of x-rays having fixed wavelength. For particular angle θ Bragg's law is satisfied and diffraction results. This method is well suited for the structure determination, when single crystal specimen is available.

2B.3.3 Powder method

The powder method of x-ray diffraction was first developed by Debye and Scherrer [13] and Hull A.W. [14] independently. This method is used in study of ferrites as the ferrite materials are polycrystalline rather than single crystal. In this method, the incident monochromatic radiation of wavelength (λ) strikes a

finely powdered specimen or a fine grained polycrystalline specimen contained in a thin walled capillary tube. The distribution of crystallites orientation will be nearly continuous. This method is most useful in the investigation of metals and alloys, where single crystals are difficult to obtain. From this method the accurate value of lattice parameter can be determined.

2B.4 Diffractometer

X-ray diffractometer can be used to analyze crystal structure. The film in the Debye Scherrer camera is replaced by a movable counter in an x-ray diffractometer. The diffractometer uses a monochromatic radiation and can be put to investigate single or polycrystalline crystals. The main features of x-ray diffractometer are shown in the Fig.(2.2).

A powder specimen `C' in the form of flat plate is mounted on a table `H' which is capable to rotate about an axis passing through `O'. The divergent beam of x-rays from the source `S' passing through the filter becomes monochromatic and is collimated by slit `A' is allowed to incident on the specimen. As the crystallites are randomly oriented, a reflection of particular position is due to a set of atomic planes

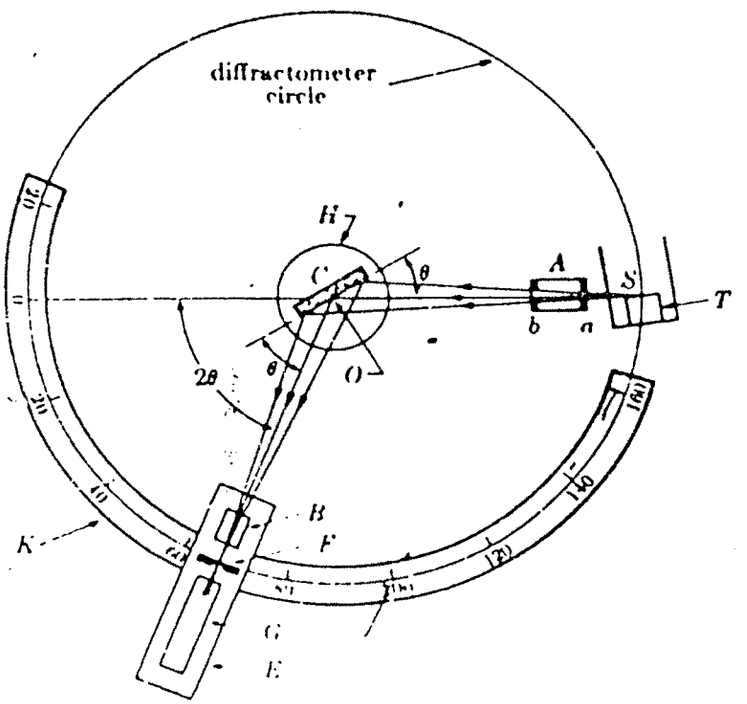

Fig. 2.2: PRINCIPLE OF THE X-RAY DIFFRACTOMETER

which satisfy Bragg's condition. The diffracted beam gets converged and focussed at slit 'F' which further enters the counter 'G' with the help of special slit 'B' the diffracted beam is then collimated. the counter G is connected to a count rate meter and output of the circuit is fed to a fast automatic recorder which registers counts per second versus 2θ.

the location of centroid of the recorded peak gives 2θ for corresponding Bragg reflection. However, in modern x-ray diffractometer proportional or scintillation counter is mounted which records automatically a graph of intensity of x-rays with respect to the Bragg's angle. The special feature of the diffractometer over Debye-Scherrer method is that it presents quantitive measure of the intensity of diffracted beam.

2B.5 Experimental

The x-ray diffraction pattern of all the samples were recorded by using CuK α radiation of wavelength 1.542 Å on Philips x-ray diffractometer. The diffraction maxima occurs when the Bragg's condition

$$2d \sin \theta = n \lambda \quad \ldots \quad 2.3$$

is satisfied.

For a cubic lattice the interplaner distance d, the lattice constant 'a' and Miller indices hkl of reflecting planes are related by [15]

$$d_{hkl} = \frac{a}{(h^2+K^2+l^2)^{1/2}} \qquad \ldots \quad 2.4$$

Substituting the value of d from equation (2.4) into equation (2.3) and rearranging we get

$$a = \frac{n\lambda}{2 \sin \theta} (h^2+K^2+l^2)^{1/2} \qquad \ldots \quad 2.5$$

using equation (2.5) lattice parameter 'a' can be calculated.

Equation (2.5) can be written for first order as

$$[h^2+K^2+l^2] = \left[\frac{4a^2}{\lambda^2}\right] \sin^2\theta \qquad \ldots \quad 2.6$$

For a particular pattern $(4a^2/\lambda^2)$ is constant. The different peaks corresponds to different values of θ, from which the value of $(h^2+K^2+l^2)$ is determined. From this value the indices hkl of each plane be written.

The bond lengths R_A and R_B are calculated by using the equation

$$R_A = (u-1/4)a\sqrt{3}$$

$$R_B = (5/8 - u)a$$

where u = Ø.381 and Ø.38Ø i.e the average value of cobalt ferrite and copper ferrite.

The radii of the ions on tetrahedral A-sites and octahedral B-sites are calculated using the formulae

$$r_A = (u-1/u)a\sqrt{3} - r(O_4^{2-})$$

$$r_B = (5/8-u)a - r(O_4^{2-})$$

2B.6 Result and discussion

The X-ray diffractograms with well defined peaks of polycrystalline samples of the $Cu_xCo_{1-x}Al_{0.5}Fe_{1.5}O_4$ system are presented in fig 2.3 to 2.8 which confirms the formation of single phase homogeneous compounds. The diffraction peaks are identified and are indexed. For all the samples (311) reflection appears to be the most intense. The other planes observed are (220) (400) (422) (333/511) and (440). These planes are allowed for cubic spinel ferrite. This confirms the formation of cubic ferrite system $Cu_xCo_{1-x}Al_{0.5}Fe_{1.5}O_4$, where x = 0, 0.2, 0.4, 0.6, 0.8 and 1. The lattice parameter and d-values are calculated for each sample. The calculated d-values agree with the observed d-values, which confirms the spinel structure. The calculated and observed d-values for different planes are shown in table 2.1 to 2.6.

The data on lattice parameters and bond lengths are given in table 2.7. The x-ray density physical

density and porosity values for the samples are listed in table 2.8.

From table 2.7 it is clear that the observed lattice parameters for copper and cobalt ferrites are in good agreement with the values reported earlier [16, 17, 18a and 18b]. It is seen that lattice parameter decreases almost linearly with addition of Cu [19]. However the sample with x = Ø.2 show higher value of lattice constant. The ionic radius of Cu and Co are Ø.7Ø A and Ø.78 A respectively. Hence there is slow decrease of lattice parameter (a) from $CoFe_2O_4$ to $CuFe_2O_4$. It seems that when Co ion from $CoFe_2O_4$ is replaced by Cu ion, there is sufficient space for Cu ion to be accommodate and hence there is contraction of lattice resulting in the decrease of lattice constant, which is seen from our observation. Similar results without aluminium for Cu-Co system have been (2Ø, 18) observed by number of workers. It is also noted that aluminium ion has smaller radius which will also affect the decrease in lattice parameter (a) values. From this table it has been observed that, there is no much variation in bond lengths Ra and Rb for all the samples.

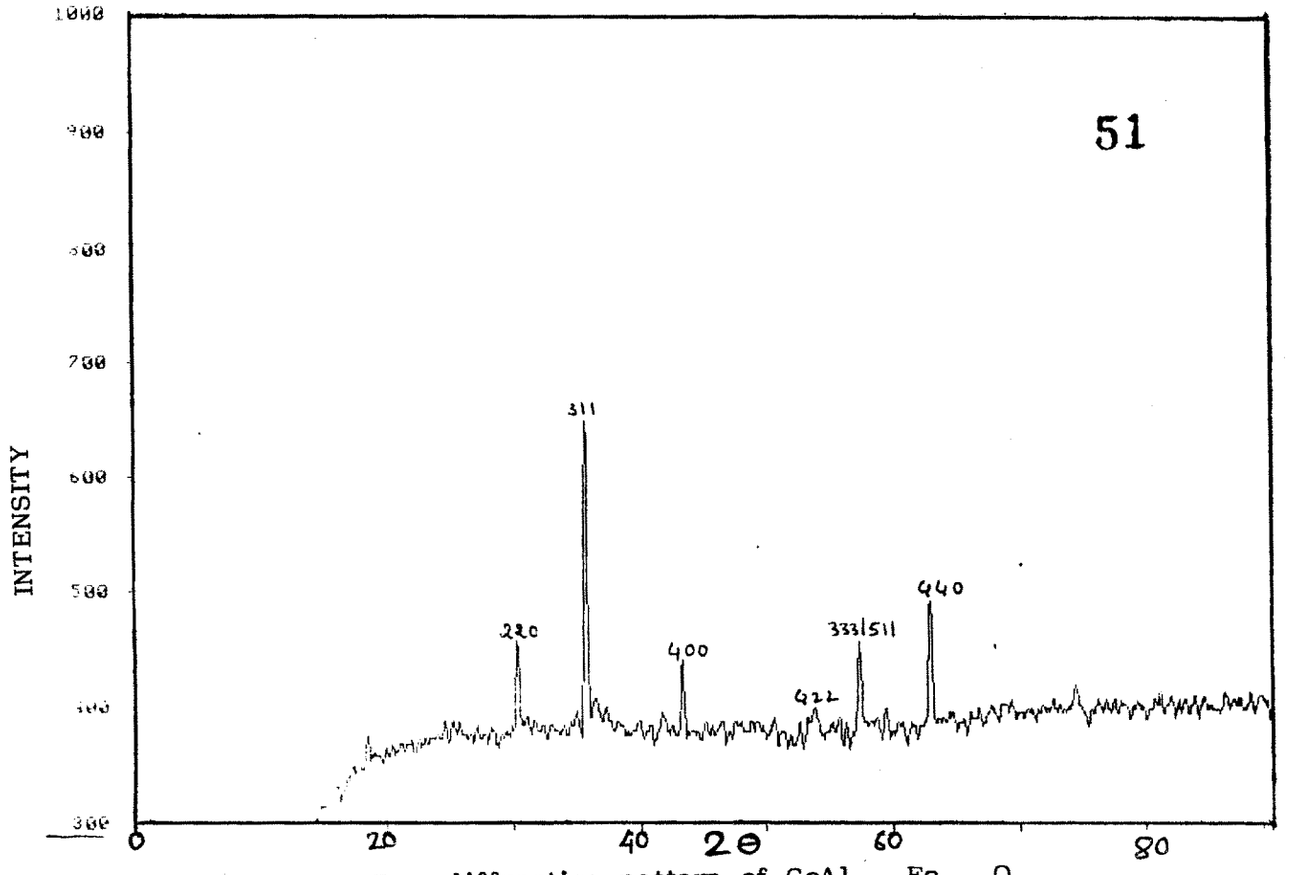

Fig.2.3 :: X-Ray diffraction pattern of $CoAl_{0.5}Fe_{1.5}O_4$

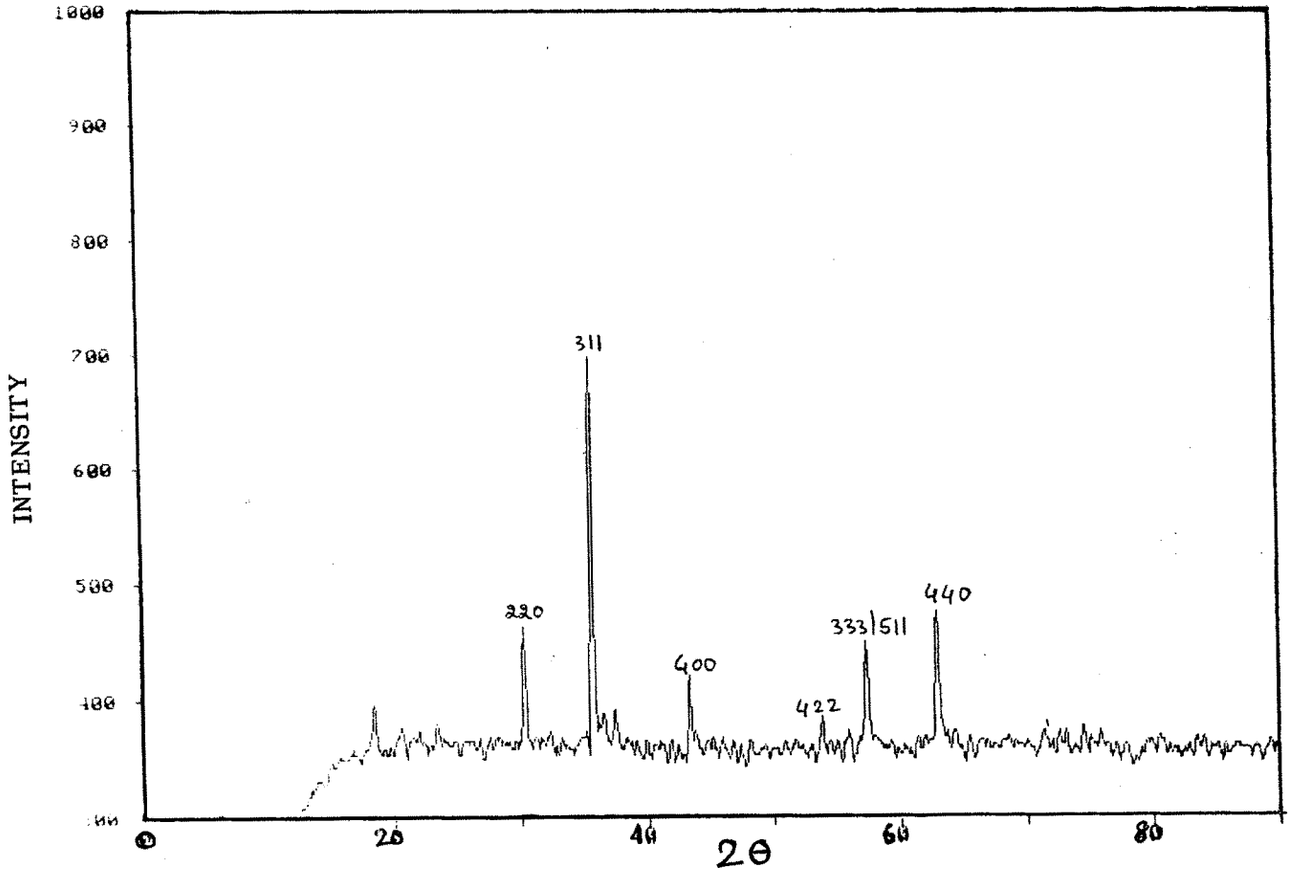

Fig. 2.4 : X-Ray Diffraction pattern of $Cu_{0.2}Co_{0.8}Al_{0.5}Fe_{1.5}O_4$

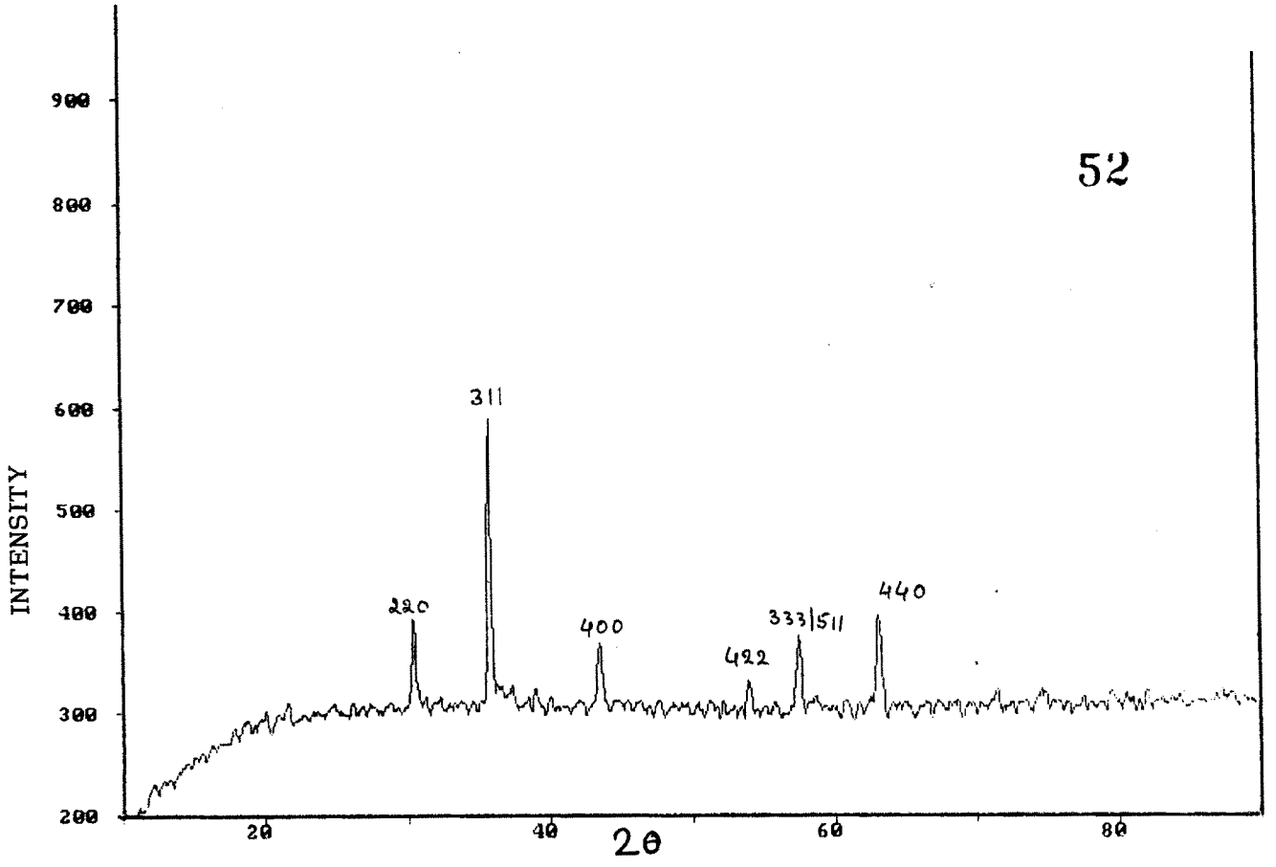

Fig.2.5 :X-Ray diffraction pattern of $Cu_{0.4}Co_{0.6}Al_{0.5}Fe_{1.5}O_4$

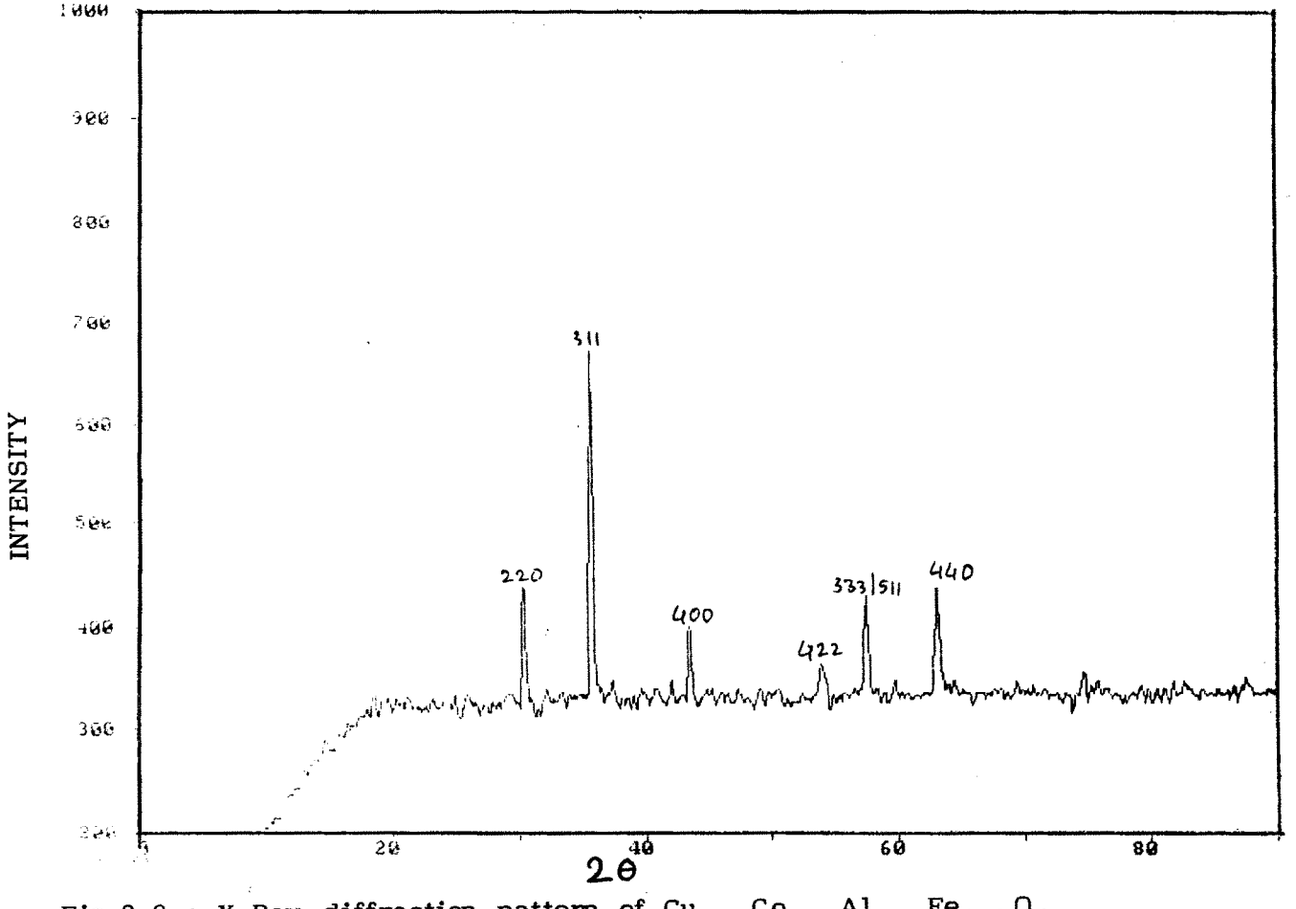

Fig.2.6 : X-Ray diffraction pattern of $Cu_{0.6}Co_{0.4}Al_{0.5}Fe_{1.5}O_4$

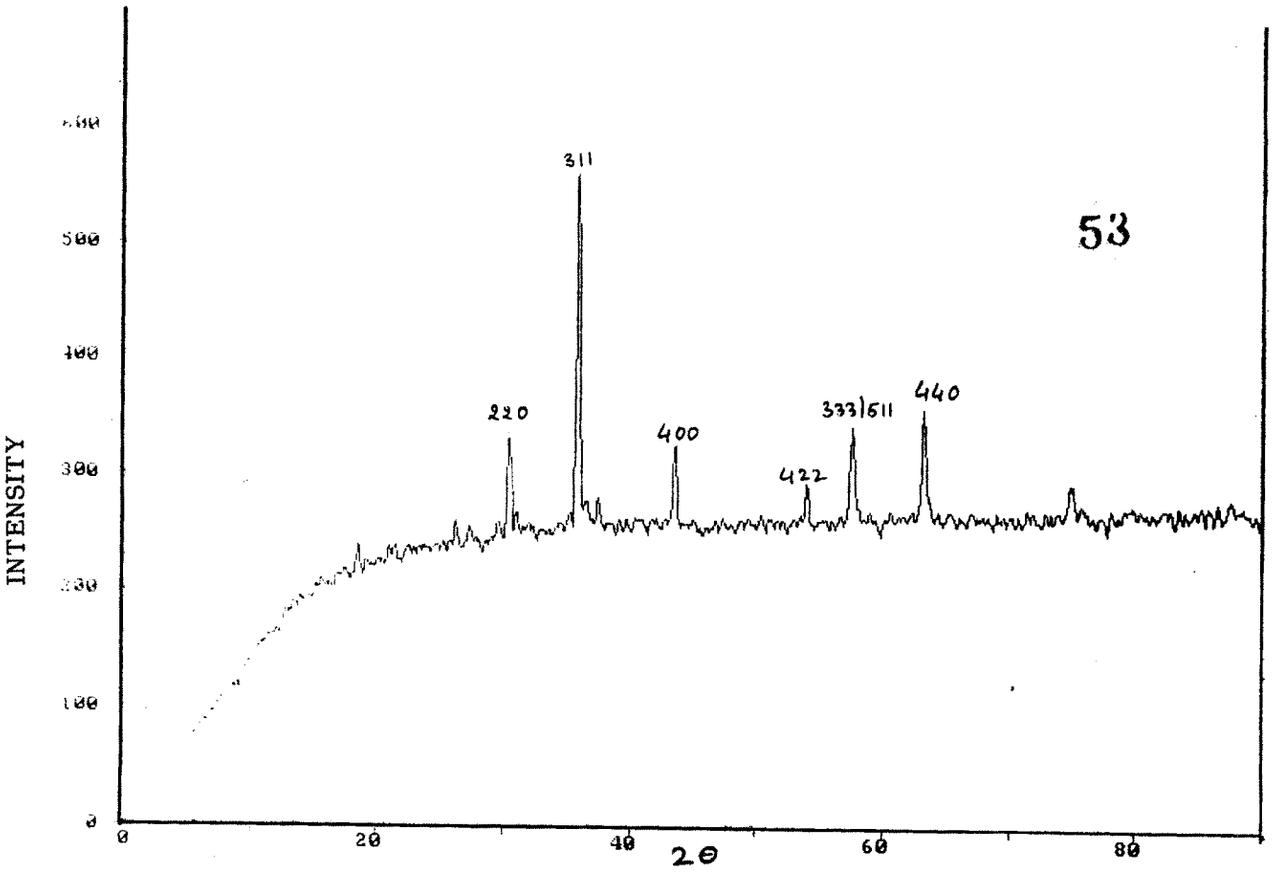

Fig.2.7 : X-Ray diffraction pattern of $Cu_{0.8}Co_{0.2}Al_{0.5}Fe_{1.5}O_4$

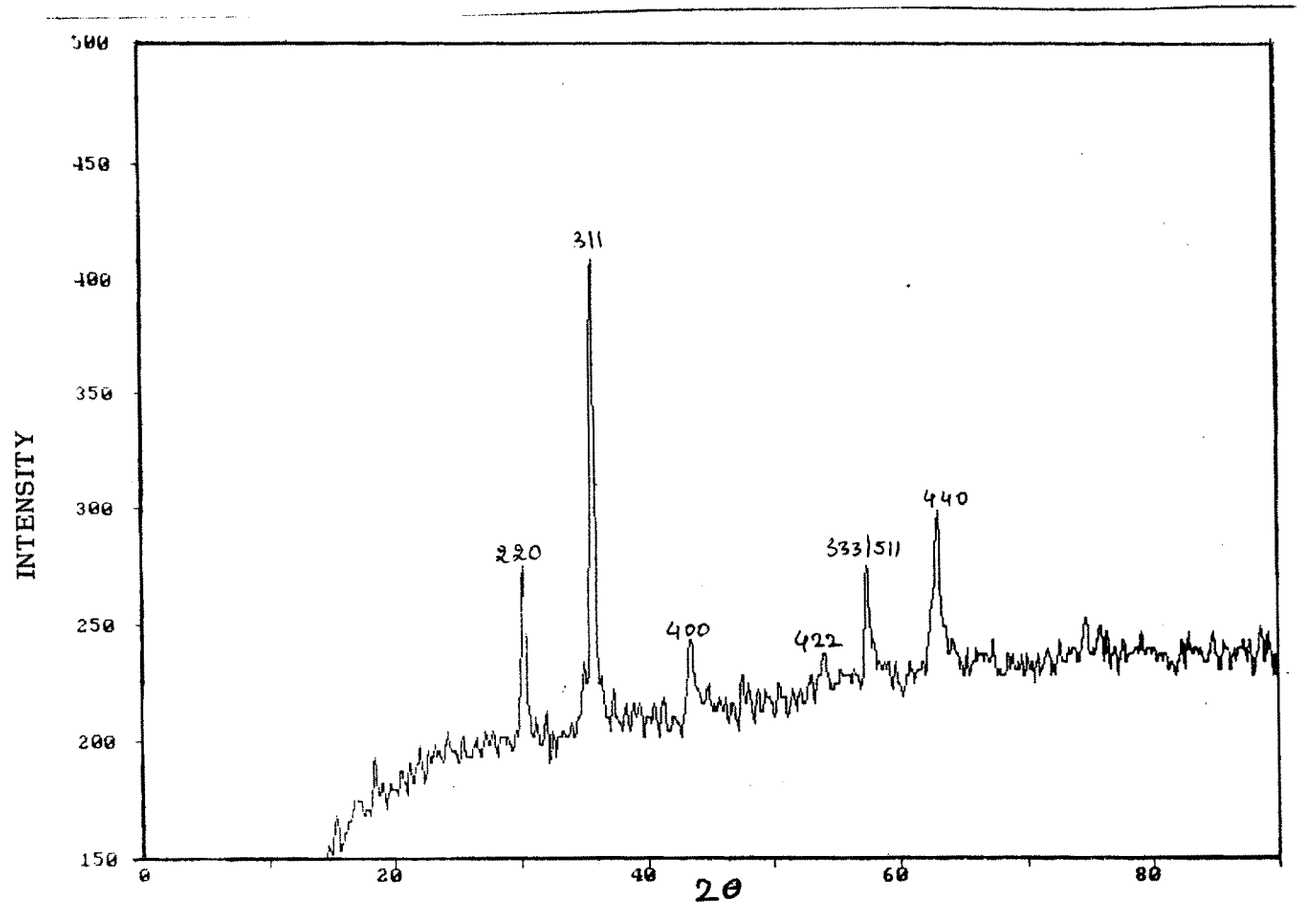

Fig.2.8 : X-Ray diffraction pattern of $CuAl_{0.5}Fe_{1.5}O_4$

Table 2.1 -X-ray diffraction data of Sample

$Co\ Al_{0.5}\ Fe_{1.5}\ O_4$
Lattice Parameter = a = 8.3421 A°

Angle 2θ	$d_{obs.}$, A°	$d_{calc.}$, A°	hkl
30.305	2.9470	2.9479	220
35.685	2.5140	2.5140	311
43.395	2.0835	2.0845	400
53.690	1.7058	1.7019	422
57.265	1.6075	1.6046	333/511
62.815	1.4782	1.4739	440

Table 2.2 -X-ray diffraction data of Sample

$Cu_{0.2}\ Co_{0.8}\ Al_{0.5}\ Fe_{1.5}\ O_4$

Lattice Parameter a = 8.3490 A°

Angle 2θ	$d_{obs.}$, A°	$d_{calc.}$, A°	hkl
30.260	2.9512	2.9522	220
35.630	2.5178	2.5176	311
43.330	2.0865	2.0875	400
53.775	1.7033	1.7044	422
57.245	1.6080	1.6069	333/511
62.905	1.4763	1.4761	440

Table 2.3 -X-ray diffraction data of Sample

$Cu_{0.4}Co_{0.6}Al_{0.5}Fe_{1.5}O_4$

Lattice Parameter a = 8.3120 A°

Angle 2θ	$d_{obs.}$, A°	$d_{calc.}$, A°	hkl
30.480	2.9304	2.9380	220
35.805	2.5059	2.5058	311
43.535	2.0772	2.0772	400
53.985	1.6972	1.6965	422
57.420	1.6035	1.5994	333/511
63.080	1.4726	1.4691	440

Table 2.4 -X-ray diffraction data of Sample

$Cu_{0.6}Co_{0.4}Al_{0.5}Fe_{1.5}O_4$

Lattice Parameter a = 8.3140 A°

Angle 2θ	$d_{obs.}$, A°	$d_{calc.}$, A°	hkl
30.385	2.9394	2.9387	220
35.800	2.5062	2.5062	311
43.480	2.0797	2.078	400
54.015	1.6963	1.6966	422
57.485	1.6019	1.5966	333/511
63.140	1.4713	1.4693	440

Table 2.5 -X-ray diffraction data of Sample

$Cu_{0.8}Co_{0.2}Al_{0.5}Fe_{1.5}O_4$

Lattice Parameter a = 8.3010 A°

Angle 2θ	$d_{obs.}$, A°	$d_{calc.}$, A°	hkl
30.515	2.9271	2.9334	220
35.865	2.5018	2.5016	311
43.575	2.0754	2.0742	400
53.970	1.6976	1.6936	422
57.485	1.6019	1.5967	333/511
63.200	1.4701	1.4667	440

Table 2.6 -X-ray diffraction data of Sample

$CoAl_{0.5}Fe_{1.5}O_4$

Lattice Parameter a = 8.3380 A°

Angle 2θ	$d_{obs.}$, A°	$d_{calc.}$, A°	hkl
30.250	2.9522	2.9483	220
35.680	2.5144	2.5143	311
43.380	2.0842	2.0847	400
57.400	1.6040	1.6048	333/511
63.055	1.4731	1.4741	440

Table 2.7

Crystallographic data of $Cu_x Co_{1-x} Al_{0.5} Fe_{1.5} O_4$

or $Cu_x Co_{1-x} Al_{2y} Fe_{2-2y} O_4$

Content x	Lattice Parameter "a" +/- 0.0037(A°)	Bond Length RA A°	RB A°
0	8.342	1.885	2.039
0.2	8.349	1.887	2.041
0.4	8.312	1.878	2.032
0.6	8.314	1.879	2.033
0.8	8.301	1.876	2.029
1	8.338	1.885	2.038

The values of lattice parameter and bond lengths of copper and cobalt ferrites without Aluminium.

Sample	a	RA	RB	Ref.
CoFe2O4	8.38	1.90	2.04	16
"	8.366	1.89	2.14	20
"	8.39	1.90	2.04	17
CuFe2O4	8.25	1.89	2.04	20, 17
"	8.27	1.80	2.08	18a
	8.32	1.79	2.06	"
	8.22	-	-	16

Table 2.8. The value of X-ray density, Physical density and Porosity data of $Cu_x Co_{1-x} Al_{2y} Fe_{2-2y} O_4$

Content x	X-ray density dx	Physical density dp	Porosity (%)
Ø	5.Ø59	3.13Ø	38
Ø.2	5.Ø46	3.284	35
Ø.4	5.135	3.4Ø8	33.5
Ø.6	5.153	3.448	33
Ø.8	5.198	4.325	16.8
1	5.151	4.621	1Ø.3

It is observed that Rb is greater than Ra for all the samples. The result is similar to other ferrite systems except cadmium ferrite for which Ra>Rb (21).

Our results on lattice parameter determined Ra and Rb with those of earlier workers without having aluminium in cobalt or copper ferrite are comparable. From the comparison it follows that there is no appreciable change by addition of Al in Ra and Rb parameter when Fe is partially replaced by Al in this ferrite system. It is because of the fact that Al which has ionic radii Al^{3+}(Ø.55 A) whereas Fe^{3+}(ionic radius = Ø.67 A). As such while replacing Fe^{3+} ions by Al^{3+} ions lattice is not disturbed as both of these ions are happen to be on B site.

From Table 2.8 it is seen that the porosity decreases with increase in copper content.

Section - C

INFRA-RED STUDIES

2C.1 Introduction

Studies of the spectral relations between structure and electromagnetic response having wavelength in the range of 1μ to 1 mm of ferromagnetic semiconductor are useful in the understanding of their properties. Since the electrical and magnetic

properties of these materials are decisively dependent on the precise configuration of atoms and ions in these structures, method of non destructive analysis such as I.R. are especially suitable to such configurations. The infrared absorption spectroscopy is an important technique to describe the local symmetries in crystalline [22] and non crystalline solids[23] and various ordering phenomenon in spinels[24,25].

In particular the vibrational, electronic and magnetic dipole spectra can give information of about the position and valency of the ions in the crystal lattice. I. R. spectroscopy when applied in the study of spinel ferrites, provides following information

1. Detection of completion of solid state reaction
2. Cation distribution (qualitatively)
3. Deformation of cubic spinel structure if any
4. Calculation of force constants

In ferrites normally, four active infrared bands are expected in the range of 100 cm^{-1} to 1000 cm^{-1}. Symmetry in spinel ferrites is O_h^7 with point group T_d and one can expect four absorption bands in the infrared region. Absorption at ν_1 is caused by stretching of tetrahedral metal and oxygen, while absorption at ν_2 is caused by vibration of oxygen in the direction perpendicular to the axis joining the tetrahedral ion

and oxygen. The remaining two bands and ν_3 and ν_4 are associated with the vibrations of metal ions in the isotropic fields of the octahedral and tetrahedral environments. But these are not observed in spinel ferrites [26]. Hafner [27], Tarte [28] and others [29] applied I.R. spectroscopy to investigate the absorption bands in many normal as well as inverse spinel ferrites. Waldron [30] and Hafner [27] assigned ν_1 band around 600 cm^{-1} to intrinsic vibrations of tetrahedral complexes and the band ν_2 around 400 cm^{-1} to octahedral complexes.

Siratori [31], Grimes et al. [32] and Kanturek et al. [33] have studied the influence exerted by cubic lattice distortion or Jahn-Teller effect on the IR spectra of spinels and the detection of these effects by means of IR spectra. Further Patakova et al. [34] have shown that the presence of Fe^{2+} ions in ferrite can cause splitting of absorption bands which is said to be due to Jahn-Teller distortion produced by Fe^{2+} ions which locally create deformation in the lattice.

2C.2 Experimental

The IR absorption spectra of six samples were recorded on Parkin-Elmer-783 IR spectrometer, at room temperature in the range of 200 cm^{-1} to 800 cm^{-1} in KBr

medium. From the IR spectra, the wave numbers ν_1 and ν_2 of absorption bands are obtained. The force constants are calculated using the relation [22].

$$K_1 = \frac{0.9421 \times [M_1 \times (\nu_2)^2]}{M_1 + 32}$$

$$U = \frac{2 \times K_1}{[\nu_1^2 \times M_1 - 2K_1]}$$

$$V = \frac{[64 - (2 \times M_1 \times U)]}{M_2}$$

$$K_2 = 0.04416 \times (\nu_1)^2 \times M_2 \times \frac{V}{V + 3}$$

where M_1 and M_2 represents the molecular weights of A and B site respectively and u and v are constants.

2C.3 Result and Discussions

The IR absorption spectra for the sample $Cu_xCo_{1-x}Al_{2y}Fe_{2-2y}O_4$ (x = 0, 0.2, 0.4, 0.6, 0.8 and 1) are shown in Figures 2C.1 to 2C.6 respectively. Table 2C.1 shows the wave numbers of different absorption bands in the samples with the force constants K_1 and K_2. The absorption spectra shows two dominant absorption bands around 610 cm^{-1} and 420 cm^{-1}. Here ν_1 corresponds to the high frequency band ranging between 590 cm^{-1} to 610 cm^{-1} and ν_2 corresponds to the low frequency band ranging between 400 cm^{-1} to 430 cm^{-1}.

Waldron [30] and Hafner [27] have attributed the bands around 600 cm^{-1} to the tetrahedral complexes and that around 400 cm^{-1} to the octahedral complexes.

In the present case, samples show two prominent absorption bands ν_1 and ν_2. It is seen from Table 2C.1 that the values of wave numbers of the bands ν_1 and ν_2 decrease with the content of copper in the samples. Apart from this the preparation conditions, grain size, porosity etc. cause the change in the values of v_1 and v_2. But the shape of the spectra suggests the possibility of splitting of 400 cm^{-1} band. The splitting of octahedral band is due to divalent metal ions on B-site. The presence of Fe^{2+} ions in the ferrite can cause splitting of the absorption band [34]. From IR spectra it is observed that the broadness of octahedral i.e. [410 ν_1] increases with increasing Cu content. This may be due to Cu ion which is a Jahn-Teller ions. The distortion at B-site due to Cu may cause fine structure or additional splitting in octahedral side. The variations in band frequencies with respect to observed values for ferrites observed by many workers may be due to preparation conditions and porosity of the material.

The force constants K_1 and K_2 are calculated from the IR absorption data using the analysis of Waldron.

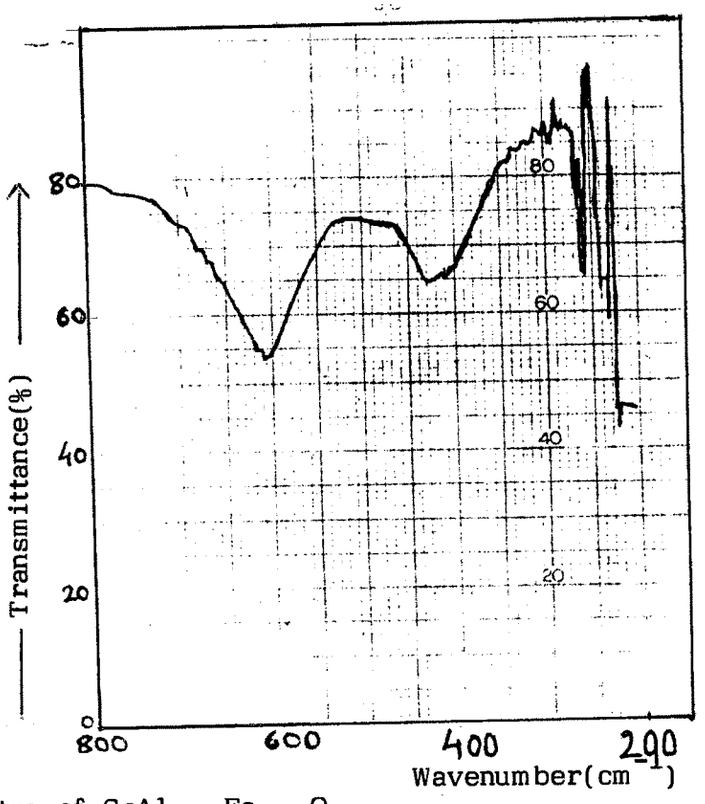

Fig.2c.1 : IR Spectra of $CoAl_{0.5}Fe_{1.5}O_4$

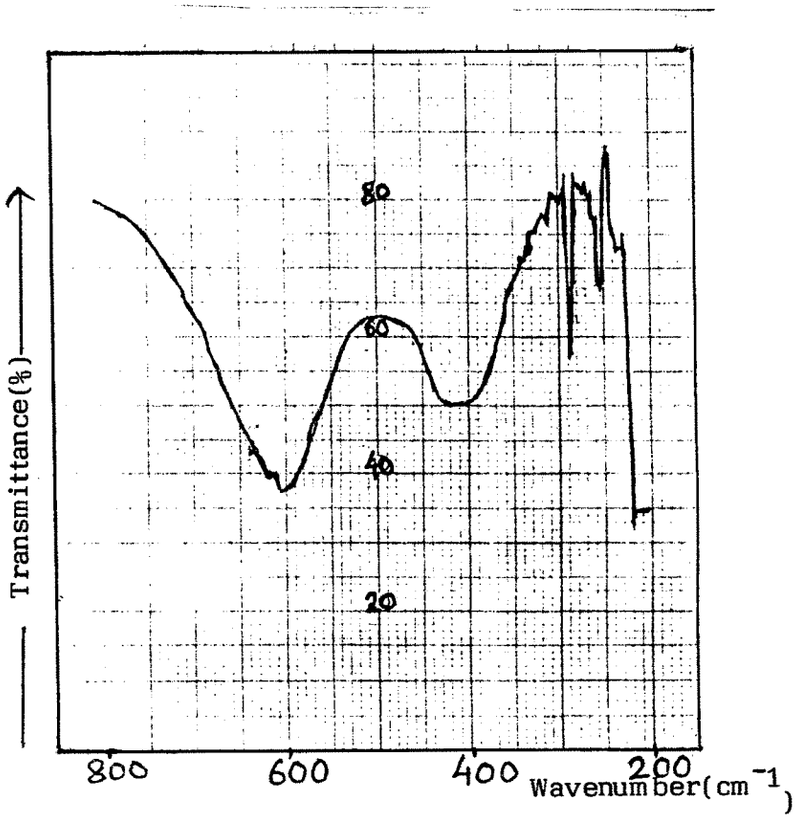

Fig.2c.2 : IR spectra of $Cu_{0.2}Co_{0.8}Al_{0.5}Fe_{1.5}O_4$

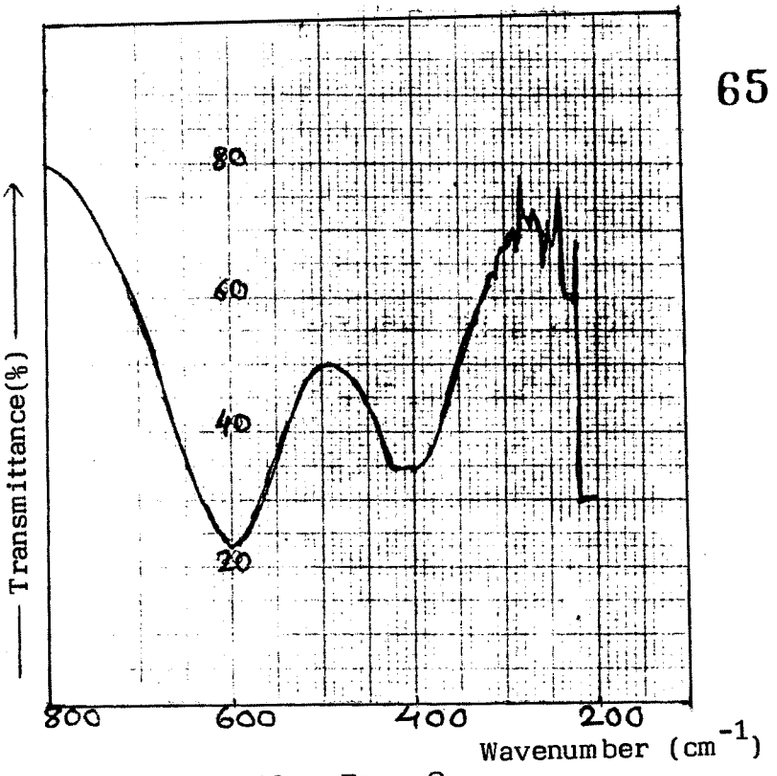

Fig.2c.3 : IR Spectra of $Cu_{0.4}Co_{0.6}Al_{0.5}Fe_{1.5}O_4$

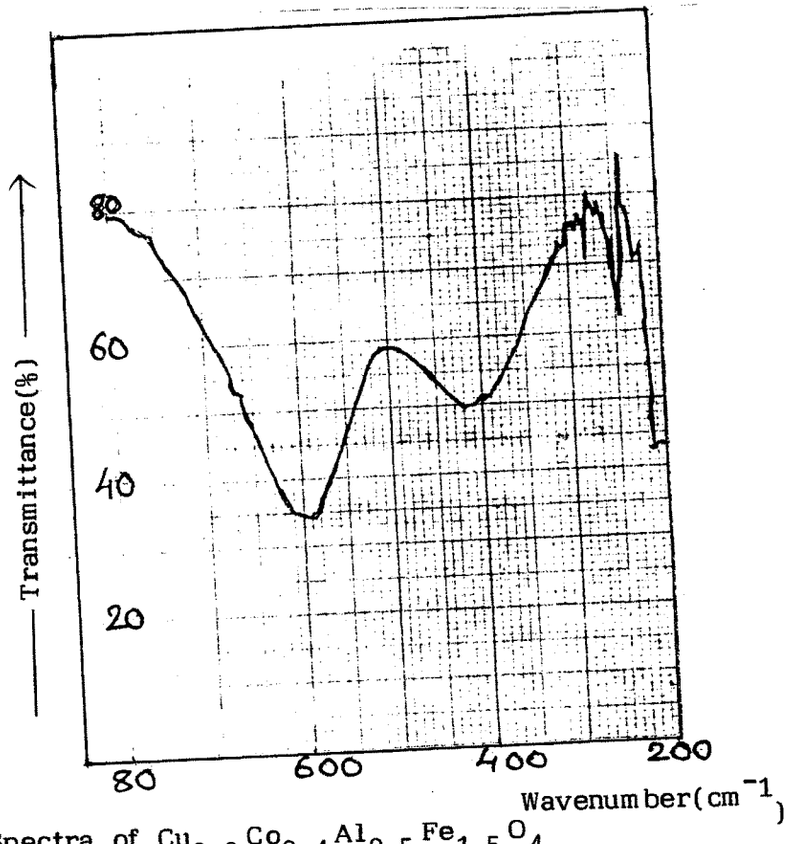

Fig.2c.4 : IR Spectra of $Cu_{0.6}Co_{0.4}Al_{0.5}Fe_{1.5}O_4$

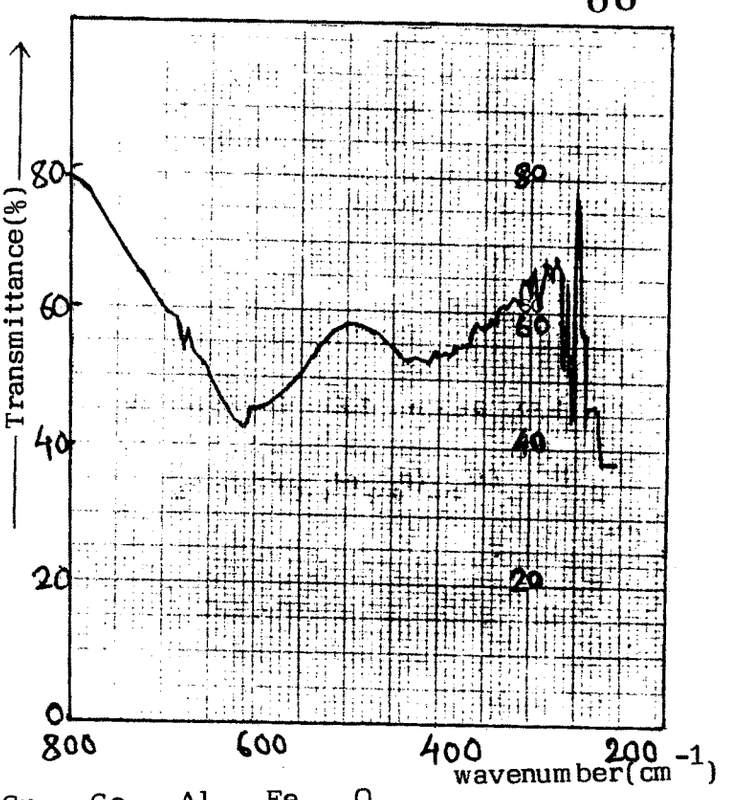

Fig.2c.5 : IR Spectra of $Cu_{0.8}Co_{0.2}Al_{0.5}Fe_{1.5}O_4$

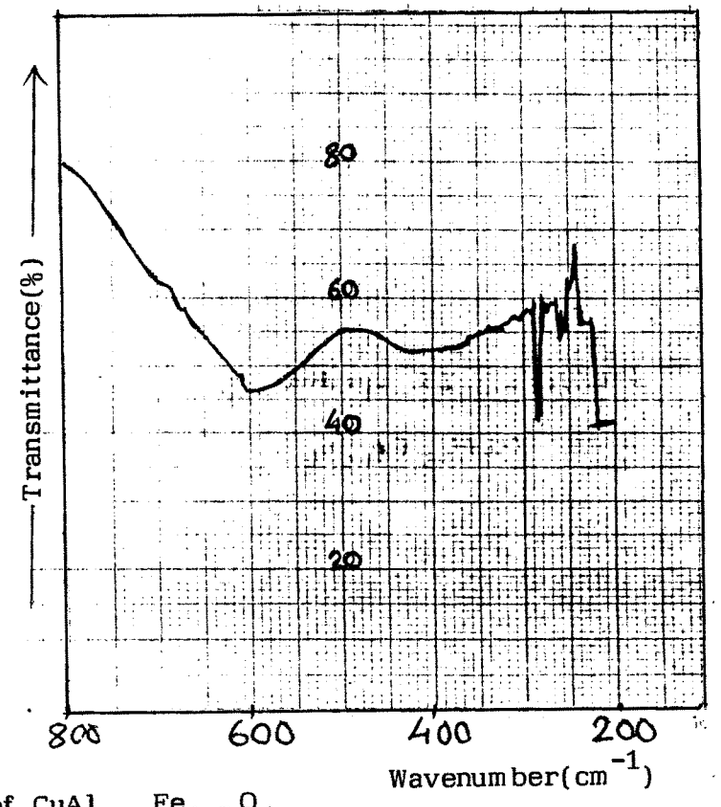

Fig.2c.6 : IR Spectra of $CuAl_{0.5}Fe_{1.5}O_4$

Table 2c.1

Band frequency and force constant for

$Cu_x Co_{1-x} Al_{2y} Fe_{2-2y} O_4$

Content	Band frequency (cm^{-1})		Force constants (dyne/cm)	
x	V_1	V_2	K_1	K_2
Ø	61Ø	43Ø	11Ø743.88	341493.42
Ø.2	61Ø	41Ø	1ØØ681.7Ø	29Ø8Ø9.2Ø
Ø.4	6ØØ	4ØØ	95831Ø.291	281774.47
Ø.6	59Ø	42Ø	1Ø5652.9	321265.2Ø
Ø.8	61Ø	41Ø	1ØØ681.7	292168.66
1	6ØØ	42Ø	1Ø5652.9	333437.58

It is observed that K_2 is greater than K_1, Srivastava et al. [35] have stated that the bond stretching for tetrahedral site would lead to higher force constant than that for the octahedral site. We also observed that tetrahedral site is more stretched than octahedral site. Cobalt makes more covalent bonds that the copper i.e. cobalt is more covalent than the copper, when we add copper to replace cobalt i.e. when copper content goes on increasing then the corresponding force constant will go on decreasing. Cobalt ferrite as well as the copper ferrite being inverse spinel the cobalt and the copper ions will be transferred to B-site and as such the force constant K_1 corresponding to B-site goes on decreasing as copper content is increased.

REFERENCES

1. Standley K.J.
"Oxide Magnetic Materials"
Clarendon Press, New York, Chapt. 2 (1962) 7

2. Magee J.H., Morton V., Fisher R.D. and Lowe I.J.
Proc. ICF Japan (1970) 217

3. Swallow D. and Jordon A.K.
Proc. Brit. Ceram. Soc. 2 (1964) 1

4. Murray P., Livey D.T. and Williams J.
"Ceramic fabrication processes"
Wiley New York p.95 (1978)

5. Leipold M.H.
"Treatise on Materials science and technology"
Ed. F.F.Y. Wand) Academic Press, New York p.95
(1976)

6. Gruntjes G.S. and Oudemans G.J.
"Special ceramics"
Ed. Popper P., Academic Press, New York p.267
(1965)

7. De Lau J.G.M.
Proc. Brit. ceram. Soc. 10 275 (1968)

8. Stuijts A.L.
Proc. ICF Tokyo Japan (1970)

9. Burke J.E.
"Kinetics of high temperature processes"
New York (1959) 109

10. Bragg W.L.
Nature, London 95 (1915) 561

11. Shull C.G. and Wollan E. and Koehlar W.C.
Phys. Rev. 84 (1952) 912

12. Prince E. and Treuting R.G.
Acta. Cryst. 9 (1956) 1025

13. Debye P. and Scherrer P.
Physica, 17 (1916) 277

14. Hull A.W.
Phys. Rev. 9 (1916) 504 and ibid. 10 (1917) 661

15. Henry N.F.M., Lipson H. and Wooster W.A.
"Interpretation of X-ray Diffraction Photographs"
McMillan and Co. Ltd, London (1961)

16. Smit J. and Wijn H.P.J.
"Ferrites"
Philips Technical Library (1959) 144

17. Patil S.I.
Ph.D. Thesis, Shivaji University, Kolhapur (1992)

18a. Namdanwadkar H.V.
M. Phil. Thesis, Shivaji University, Kolhapur
(1989)

18b. Kulkarni B.M.
M. Phil. Thesis, Shivaji University, Kolhapur
(1995)

19. Verwey E.J.W. and Heilman E.L.
J. Chem. Phys. 15 174 (1947)

20. Kamble P.N., Medikeri T.B. and Kolekar C.B.
M. Phil. and Ph. D. theses, Shivaji University,
Kolhapur (1994)

21. Upadyay R.V. and Kulkarni R.G.
Solid State Commun. 48 (1983) 691

22. Gawade R.J.
Ph. D. Thesis, Shivaji University, Kolhapur (1993)

23. Simsa Z., Simsova J. and Brabers V.A.M.
Proc. XI Intnl. Conf. on Progress in
Semiconductors, Warsaw, Poland 2 (1072) 1294

24. Rezlescu N. and Rezlescu E.
Solid State Commun.(USA) 14 (1974) 69

25. Kulkarni V.R., Todkar M.M. and Vainganakar A.S.
Ind. J. Pure and Applied Physics 24 (1986) 294

26. Satomi K.J.
Phys. Soc. Japan 16 91961) 258

27. Hafner S.
Z. fur Krist 115 331(2) (1961)

28. Tarte P.
Spectrochim. Acta. 21 (1965) 313

29. White W.B. and De Angelis B.A.
Spectrochim. Acta Vol.A (GB) 23 (1967) 985

30. Waldron R.D.
Phys. Rev. (USA) 99 (1955) 1727

31. Siratori Kiitti
J. Phys. Soc. Japan 23 (1967) 848

32. Grimes N.W. and Collet A.
Phys. Stat. Solidi (b) 43 (1971) 591

33. Kanturek J. and Simsa Z.
Phys. Stat. Solidi 36 (1969) 47

34. Potakova V.R., Zervey N.D. and Romanov V.P.
Phys. Stat. Solidi (a) (Germ) 12 (1972) 623

35. Srivastava C.M. et al
J. Appl. Phys. 53 (1982) 8184